Hydrogen Bonding in Nitroanilines: Neutron Diffraction Study of *m*-Nitroaniline at 100 K

Andrés E. Goeta,*,† Chick C. Wilson,‡ Juan C. Autino,§ Javier Ellena,‖,⊥ and
Graciela Punte‖

*Department of Chemistry, University of Durham, Durham, DH1 3LE, United Kingdom,
ISIS, Rutherford Appleton Laboratory, Chilton, Didcot, Oxon, OX11 0QX, United Kingdom,
LADECOR, Departamento de Química, Facultad de Ciencias Exactas, Universidad Nacional
de La Plata, 47 y 115, B1900 AJL La Plata, Argentina, IFLP & LANADI, Departamento de
Física, Facultad de Ciencias Exactas, Universidad Nacional de La Plata, CC 67, B1900 ZAA,
La Plata, Argentina, and Departamento de Física e Informática, Instituto de Física de São
Carlos, Universidade de São Paulo, C. P. 369, 13560-970, São Carlos, SP, Brazil*

An appreciable degree of pyramidalization of the amine nitrogen atom is observed in the title compound. The existence of polar chains, induced by N−H···O synthons and stabilized by a C(ar)−H···O interaction, is confirmed. An N−H···N interaction, disregarded in molecular orbital calculations, was found to stabilize even further the known head-to-head assembling of the chains and to be responsible for the polar layer's formation. The structure can be described as polar layers on the *bc* plane, embodying chains interlinked by N−H···N interactions and connected by weak C(aryl)−H···O interactions.

Introduction

Much effort has been devoted in the past decade to the study, design, and understanding of the aggregation of organic molecules.[1−5] The considerable interest in the field has been based on the fact that crystal engineering, the ability to predict or direct the three-dimensional arrangement, can be used to tailor materials of biological or technological importance.[6] In this context, intermolecular hydrogen bonds are an effective tool for organizing organic molecules, very well typified by nitroaniline compounds, which associate via intermolecular H-bonds between the amino and nitro groups.

The main interest in nitroanilines comes from their recognized second harmonic generation capability and their large microscopic hyperpolarizabilities. In particular, *m*-nitroaniline (mNA) has been the subject of many studies because of its relatively simple molecular structure[7,8] and large electrooptic effect[9−11] and nonlinear

optic effects.[12−23] Furthermore, mNA has been found recently to show piezoelectric[24] and ferroelectric[25] behaviors. The nonlinear responses of crystals have their origin in their molecular nonlinearities, but the relative orientation of the molecules, induced by crystal packing, plays a crucial role in crystal nonlinear efficiency. In particular, second harmonic generation is impaired if the molecular arrangement in the crystal is centrosymmetric. In so-called molecular crystals, the relationship between molecular and macroscopic properties have been modeled, up to the present, by the oriented-gas formalism.[26,27] However, some recent results[28,29] would indicated that packing forces and intermolecular inter-

* To whom correspondence should be addressed. E-mail: A.E.Goeta@durham.ac.u.
† University of Durham.
‡ Rutherford Appleton Laboratory.
§ Departamento de Química.
‖ Departamento de Física.
⊥ Universidade de São Paulo.

(1) Turi, L.; Dannenberg, J. J. *J. Phys. Chem.* **1993**, *97*, 12197 and references therein.
(2) Turi, L.; Dannenberg, J. J. *J. Phys. Chem.* **1995**, *99*, 639 and references therein.
(3) Turi, L.; Dannenberg J. J. *J. Phys. Chem.* **1996**, *100*, 9638 and references therein.
(4) Desiraju, G. R. *Acc. Chem. Res.* **1996**, *29*, 441.
(5) Aakeröy, C. B. *Acta Cryst. B* **1997**, *53*, 569.
(6) Desiraju, G. R. *J. Chem. Soc., Chem. Comm.* **1997**, 1471 and references therein.
(7) Skapski, A. C.; Stevenson, J. L. *J. Chem. Soc., Perkin Trans. 2* **1973**, 1197.
(8) Ploug-Sorensen, G.; Krogh Andersen, E. *Acta Cryst. C* **1986**, *42*, 1813.
(9) Kalymnios, D. *J. Phys. D* **1972**, *5*, 667.

(10) Stevenson, J. L. *J. Phys. D* **1973**, *6*, L13.
(11) Ayer, S.; Faktor, M. M.; Marr, D.; Stevenson, J. L. *J. Mater. Sci.* **1972**, *7*, 31.
(12) Bokut, B. V. *J. Appl. Spectrosc.* **1967**, *7*, 425.
(13) Southgate, P. D.; Hall, D. S. *Appl. Phys. Lett.* **1971**, *18*, 456.
(14) Southgate, P. D.; Hall, D. S. *J. Appl. Phys.* **1972**, *43*, 2765.
(15) Davydov, B. L.; Koreneva, L. G.; Lavrovskii, E. A. *Radio. Eng. Electron. Phys.* **1974**, *19*, 6, 130.
(16) Oudar, J. L.; Chemla, D. S. *J. Chem. Phys.* **1977**, *66*, 2664.
(17) Oudar, J. L.; Hierle, R. *J. Appl. Phys.* **1977**, *48*, 2699.
(18) Carenco, A.; Jerphagnon J.; Perigaud, A. *J. Chem. Phys.* **1977**, *66*, 3806.
(19) Bergman, J. G.; Crane, G. R. *J. Chem. Phys.* **1977**, *66*, 3803.
(20) Kato, K. *IEEE J.* **1980**, *QE−16*, 1288.
(21) Roberts, D. A. *IEEE J.* **1992**, *QE−28*, 2057.
(22) Dmitriev, V. G.; Nikogosyan, D. N. *Opt. Commun.* **1993**, *95*, 173.
(23) Huang, G.-F.; Lin, J. T.; Su, G.; Jiang, R.; Xie, S. *Opt. Commun.* **1992**, *89*, 205.
(24) Avanci, L. H.; Cardoso, L. P.; Girdwood, S. E.; Pugh, D.; Sherwood, J. N.; Roberts, K. J. *Phys. Rev. Lett.* **1998**, *81*, 5426.
(25) Avanci, L. H.; Braga, R. S.; Cardoso, L. P.; Galvão, D. S.; Sherwood, J. N. *Phys. Rev. Lett.* **1999**, *83*, 5146.
(26) Chemla, D. S.; Oudar, J. L.; Jerphagnon, J. *Phys. Rev. B* **1975**, *15*, 4534.
(27) Zyss, J.; Oudar, J. L. *Phys Rev. A* **1982**, *26*, 2028.
(28) Isaacs, E. D.; Shukla, A.; Platzman, P. M.; Hamann, D. R.; Barbiellini, B.; Tulk, C. A. *Phys. Rev. Lett.* **1999**, *82*, 600.
(29) Espinosa, E.; Souhassou, M.; Lachekar, H.; Lecomte, C. *Acta Cryst. B* **1999**, *55*, 563.

actions in the crystal will play a crucial part in the final macroscopic properties of these materials. So, understanding these intermolecular interactions should help toward understanding the nature of the macroscopically produced effects.

Analysis of X-ray data from a series of nitroanilines has shown the existence of polar chains as a common structural feature, giving rise to the assumption that N−H···O(nitro) synthons in nitroanilines are so strong that they induce molecules to assemble in polar chains as the first aggregation step in solution, which in turn would induce the formation of acentric structures during the crystal nucleation.[30,31] In the same works, it was proposed that the hydrogen bonding forming these chains will have an asymmetric bifurcated motif. Several semiempirical and ab initio calculations on aniline derivative aggregates have been performed with the aim of rationalizing these assumptions and examining the validity of the oriented-gas formalism.[3,32,33] However, such rationalization has not been possible, and the latter has been seriously questioned.[33] This failure has been partially ascribed to the omission of the nonplanarity of the amino group in most calculations,[34] which in turn has probably been due mainly to the lack of reliable experimental diffraction and gas-phase spectroscopic data. Moreover, amino group planarity has been supported by most organic textbook descriptions[35,36] and even by surveys of the geometries of unsubstituted[37] and substituted aromatic amines.[38] However, later ab initio studies performed on the aniline-free molecule[34,39] and the neutron diffraction structure determinations of 2- and 3-aminophenols[40] and 2-methyl-5-nitroaniline[41] have provided evidence of nonplanarity.

X-ray data on 2-methyl-4-nitroaniline (2M4NA)[42] shows a hydrogen bond (HB) scheme that follows the description of Etter et al.[31] Low-temperature neutron diffraction studies of the isomeric 2-methyl-5-nitro-aniline (2M5NA)[41] have shown a similar chain motif, despite the presence of hydrogen-bonded centrosymmetric dimers, which rules against noncentric packing, and nonconventional hydrogen bonds stabilizing its three-dimensional structure. To clarify the relationship between the different parameters which appear to influence the self-assembly of nitroanilines, additional reliable data on hydrogen positions must be obtained.

In the case of mNA, conflicting hydrogen bond schemes have been proposed in the literature to explain the observed crystal growth and morphology dependence on the solvents employed[43] and to rationalize crystal packing.[3,30] Besides, recent DSC measurements would indicate the existence of a phase transition at 160 K.[44] For these reasons, a low-temperature single-crystal neutron diffraction study of mNA has been performed. The aim of this study is to add to the understanding of the role of the hydrogen bonds in the molecular organization of mNA in particular and of nitroanilines in general. In addition, the reliable H atoms positions thus obtained can be the starting point for either an electron distribution study or aggregate calculations that would allow an understanding of the properties of mNA crystals and to verify the reliability of the additivity model. Validation of the additivity model is crucial for materials design.

Experimental Section

The compound, purchased from a commercial source (Fluka), was purified by recrystallization, first from methanol and then from benzene hot saturated solutions, by cooling them to 5 °C. The polycrystalline material obtained was dissolved in a small amount of anhydrous (sodium benzophenone dried) dioxane, so that a saturated solution at about 24 °C was obtained. A crystal of approximate dimensions $10 \times 2 \times 2$ mm was then carefully grown by using a thermostatic bath (Selecta Frigiterm S-382), lowering the temperature at a rate of 0.1 °C/8 h down to about 21 °C.

The crystal thus grown was used to collect neutron diffraction data on the SXD instrument at the ISIS spallation neutron source, using the time-of-flight Laue diffraction method.[45] Experimental conditions have been described previously and were the same as those for 2M5NA.[41] The intensities were extracted and reduced to structure factors using standard SXD procedures.[45] A total of 11 625 reflections were observed, reducing to a unique set of 1664 structure factors on merging ($R_{int} = 0.06$). This structure factor set was used for structural refinement in SHELXL-93.[46] All non-hydrogen atoms positions from the X-ray model were used as a starting point for the refinement. Hydrogen atom positions were located from subsequent difference Fourier maps. All atoms refined with anisotropic displacement parameters. Neutron scattering lengths were taken from *International Tables for Crystallography,* Vol. C, Table 4.4.4.1. Crystal data and a summary of the data collection and refinement parameters are given in Table 1. Final atomic positions are given in Table 2, and bond distances and angles are given in Table 3.

Discussion

The planarity of the amino group was analyzed through the examination of two internal coordinates, τ and χ_N, after Ferretti et al.[47] These are a function of the torsion angles involving the hydrogen atoms: $\omega_1 =$ C6−C1−N1−H11 $= -20.9(5)°$, $\omega_2 =$ C2−C1−N1−H12 $= 23.4(5)°$, $\omega_3 =$ C2−C1−N1−H11 $= 162.1(5)°$ and $\omega_4 =$ C6−C1−N1−H12 $= -159.6(5)°$. τ $(0 \le \tau \le 90°) = (\omega_1$

(30) Panunto, T. W.; Urbánczyk-Lipkowska, Z.; Johnson, R.; Etter, M. C. *J. Am. Chem. Soc.* **1987**, *109*, 7786.

(31) Etter, M. C.; Frankenbach, G. M.; Adsmond, D. A. *Mol. Cryst. Liq. Cryst.* **1990**, *187*, 25.

(32) Dannenberg, J. J. *ACS Symp. Ser.* **1991**, *455*, 457.

(33) Hamada, T. *J. Phys. Chem.* **1996**, *100*, 8777.

(34) Bludsky, O.; Sponer, J.; Leszczynski, J.; Špirko, V.; Hobza, P. *J. Chem. Phys.* **1996**, *105*, 11042.

(35) Morrison, R. T.; Boyd, R. N. *Organic Chemistry*, 5th ed.; John Wiley: New York, 1987.

(36) Fessenden, R. J.; Fessenden, J. S. *Organic Chemistry*, 4th ed.; Brooks-Cole: California, 1990.

(37) Allen, F. H.; Davies, J. E.; Galloy, J. J.; Johnson, O.; Kennard, O.; Macrae, C. F.; Mitchell, E. M.; Mitchell, G. F.; Smith, J. M.; Watson, D. G. *J. Chem. Inf. Comput. Sci.* **1991**, *31*, 187.

(38) Allen, F. H.; Bird, C. M.; Rowland, R. S.; Harris, S. E.; Schwalbe, C. H. *Acta Cryst. B* **1995**, *51*, 1068.

(39) Adams, D. B. *J. Chem. Soc., Perkin Trans. 2* **1993**, 567.

(40) Allen, F. H.; Hoy, V. J.; Howard, J. A. K.; Thallandi, V. R.; Desiraju, G. R.; Wilson, C. C.; McIntyre G. J. *J. Am. Chem. Soc.* **1997**, *119*, 3477.

(41) Ellena, J.; Goeta, A. E.; Howard, J. A. K.; Wilson, C. C.; Autino, J. C.; Punte, G. *Acta Crystallogr. B* **1999**, *55*, 209.

(42) Howard, S. T.; Hursthouse, M. B.; Lehmann, C. W.; Mallinson, P. R.; Frampton, C. S. *J. Chem. Phys.* **1992**, *97*, 5616.

(43) Cang, H. X.; Huang, W. D.; Zhou, Y. H. *J. Cryst. Growth* **1998**, *192*, 236.

(44) Szostak, M. M.; Wójcik, G.; Gallier, J.; Bertault, M.; Freundlich, P.; Kolodziej, H. A. *Chem. Phys.* **1998**, *229*, 275.

(45) Wilson, C. C. *J. Mol. Struct.* **1997**, *405*, 207.

(46) Sheldrick, G. M. *SHELXL-93* (A program for the refinement of single-crystal diffraction data) University of Göttingen: Germany, 1993.

(47) Ferretti, V.; Bertolasi, P.; Gilli, P.; Gilli, G. *J. Phys. Chem.* **1993**, *97*, 13568.

Table 1. Experimental Details

Crystal Data

chemical formula	$C_6H_6N_2O_2$
chemical formula weight	138
cell setting	orthorhombic
space group	$Pca2_1$
a (Å)	18.905(4)
b (Å)	6.484(1)
c (Å)	5.016(1)
V (Å^3)	614.9(2)
Z	4
D_x (Mg m^{-3})	1.491
radiation type	neutron
wavelength range (Å)	0.5–5
μ (cm^{-1})	$0.82 + 0.79\,\lambda$
temperature (K)	100
crystal form	prismatic needle
crystal size (mm)	$10 \times 2 \times 2$
crystal color	orange

Data Collection

radiation source	ISIS
diffractometer	SXD
data collection method	time-of-flight Laue diffraction
absorption correction	empirical
T_{min}	0.43
T_{max}	0.81
no. of measured reflections	11 625
no. of unique reflections	1664
no. of observed reflections	1664
$[I > 2\sigma(I)]$	
R_{int}	0.060
range of h, k, l	0–38, 0–13, −10−0

Refinement

$R\ [F^2 > 2\sigma(F^2)]$	0.0529
w$R(F^2)$	0.1377
S	1.117
no. of reflections used in the refinement	1664
no. of parameters refined	145
H-atom treatment	all H-atom param. refined
extinction method	Becker-Coppens Lorentzian model
extinction coefficient	0.127

Table 2. Atomic Coordinates and Equivalent Isotropic Displacement Parameters (Å^2) for mNA

	x	y	z	U_{eq}
C1	0.1517(1)	1.0450(3)	0.1792(3)	0.014(1)
C2	0.0916(1)	1.0156(3)	0.0205(4)	0.018(1)
C3	0.0487(1)	0.8448(4)	0.0531(4)	0.020(1)
C4	0.0643(1)	0.6960(3)	0.2440(4)	0.017(1)
C5	0.1242(1)	0.7283(3)	0.3985(3)	0.013(1)
C6	0.1683(1)	0.8975(3)	0.3714(4)	0.014(1)
N1	0.1958(1)	1.2117(2)	0.1389(3)	0.020(1)
N2	0.1416(1)	0.5766(2)	0.6024(3)	0.018(1)
O1	0.1012(2)	0.4316(5)	0.6349(8)	0.033(1)
O2	0.1952(2)	0.5999(5)	0.7348(7)	0.029(1)
H2	0.0785(4)	1.1276(10)	−0.1304(14)	0.040(1)
H3	0.0022(4)	0.8277(12)	−0.0675(14)	0.044(1)
H4	0.0316(3)	0.5610(9)	0.2740(14)	0.037(1)
H6	0.2146(3)	0.9134(9)	0.4962(13)	0.035(1)
H11	0.2281(3)	1.2447(9)	0.2917(13)	0.036(1)
H12	0.1748(3)	1.3348(8)	0.0489(14)	0.036(1)

$+ \omega_2)/2$, characterizes the rotation around the C1−N1 bond and χ_N $(0 \leq \chi_N \leq 60°) = \omega_2 - \omega_3 + \pi(\text{mod. } 2\pi)$ is a measure of the degree of the nitrogen atom pyramidalization (P_N). The extreme values, 0° and 60°, correspond to a planar sp^2 and a regular tetrahedral sp^3 hybridized nitrogen, respectively. The values obtained in the present work, $\tau = 1.3$ (5)° and $\chi_N = 41.3$ (5)°, indicate a slight rotation and a significant P_N. The P_N can be also assessed from the nitrogen atom distance to the plane made by its substituents (H11, H12, C1), 0.238(4) Å, and the sum of the angles about the amino

Table 3. Intramolecular Bonds Distances (Å) and Angles (°)

C1−N1	1.380(2)	C3−C2−H2	119.2(4)
C1−C6	1.394(2)	C1−C2−H2	119.5(4)
C1−C2	1.401(3)	C2−C3−C4	120.8(2)
C2−C3	1.382(3)	C2−C3−H3	119.8(4)
C2−H2	1.078(6)	C4−C3−H3	119.4(4)
C3−C4	1.391(3)	C5−C4−C3	116.9(2)
C3−H3	1.072(6)	C5−C4−H4	120.8(4)
C4−C5	1.388(3)	C3−C4−H4	122.3(4)
C4−H4	1.083(5)	C6−C5−C4	123.8(2)
C5−C6	1.384(2)	C6−C5−N2	117.9(2)
C5−N2	1.457(2)	C4−C5−N2	118.3(2)
C6−H6	1.082(6)	C5−C6−C1	118.5(2)
N1−H11	1.003(6)	C5−C6−H6	120.4(4)
N1−H12	1.000(5)	C1−C6−H6	121.1(4)
N2−O2	1.221(3)	C1−N1−H11	115.0(4)
N2−O1	1.223(3)	C1−N1−H12	116.8(4)
N1−C1−C6	120.2(2)	H11−N1−H12	114.7(5)
N1−C1−C2	120.9(2)	O2−N2−O1	122.7(2)
C6−C1−C2	118.8(2)	O2−N2−C5	119.1(2)
C3−C2−C1	121.2(2)	O1−N2−C5	118.2(2)

Table 4. Hydrogen Bonding Geometry[a]

	D−H (Å)	H···A (Å)	D···A (Å)	D−H···A (°)
N1−H12···O1′	1.000(5)	2.577(7)	3.409(4)	140.7(5)
N1−H12···O2′	1.000(5)	2.364(6)	3.232(3)	144.8(5)
N1−H11···N1″	1.003(6)	2.268(6)	3.238(2)	162.2(5)
C2−H2···O1′	1.078(6)	2.335(6)	3.324(3)	151.7(5)
C4−H4···O1‴	1.083(5)	2.605(7)	3.283(4)	120.0(4)

[a] Symmetry codes: (′) x, $1 + y$, $z − 1$; (″) $^1/_2 − x$, y, $^1/_2 + z$; (‴) $−x$, $1 − y$, $z − ^1/_2$.

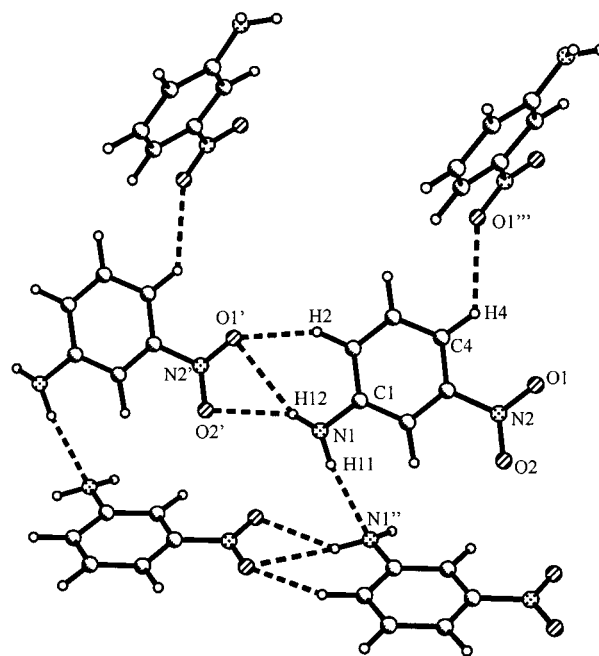**Figure 1.** Illustration of the intermolecular hydrogen bonding pattern in nMA.

nitrogen, 346.5(10)°. However, a partial amino group planarization has been related to an enhancement of conjugation due to intermolecular interactions inducing cooperative effects,[3,48] and hence, these interactions were analyzed carefully.

Intermolecular distances found in this neutron study of mNA (see Table 4 and Figure 1) show that the H12 aminic hydrogen is connected with the two oxygens of

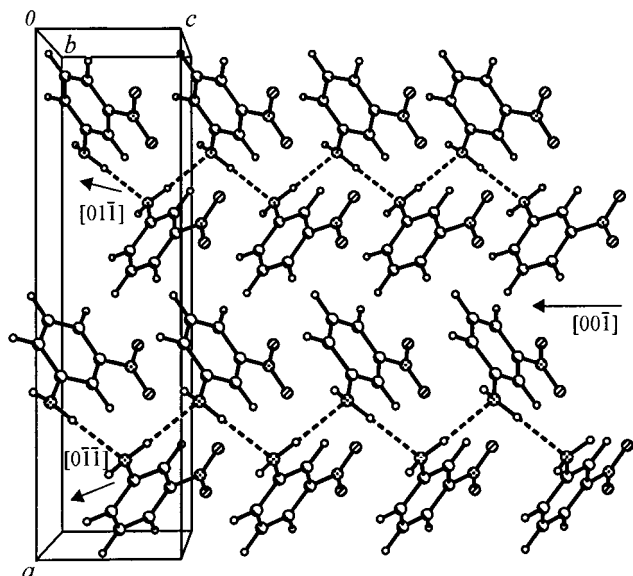(48) Ellena, J. Ph.D. Thesis, Universidad Nacional de La Plata, Argentina, 1998.

Figure 2. View of mNA polar ribbons, with chains either along [01$\bar{1}$] or [0$\bar{1}\bar{1}$], originating the polar layers.

a nitro group through an asymmetric bifurcated HB in accordance with Panunto et al.[30] This motif is however, more symmetric than the one found in 2M5NA. This N−H···O(nitro) interaction connects molecules related by a translation operation and induces the formation of infinite polar chains along [01$\bar{1}$] and [0$\bar{1}\bar{1}$] where consecutive molecules are parallel to each other. Molecules in the chain are also joined by a C(ar)−H···O interaction, as shown in Figure 1. This type of interaction motif has been previously outlined by Dannenberg[32] from molecular orbital modeling of monomeric aggregates in mNA. Contrary to the case of 2M5NA dimers are not formed here, instead chains associate in pairs to form polar ribbons. The association is induced by a significant N−H···N interaction (see Table 4), not reported previously, which links molecules with their mean planes forming an angle of 66.70(6)° between them (Figure 1) and related by a glide operation. The ribbons stack to originate a polar layer with chains either along [01$\bar{1}$] or [0$\bar{1}\bar{1}$], and the three-dimensional structure can be described as polar layers piled along *a* as shown in Figure 2. Adjacent layers, alternately comprising chains oriented along [01$\bar{1}$] and [0$\bar{1}\bar{1}$], are connected via a weak C(ar)−H···O bond, and all in all we have a polar supermolecule along the [00$\bar{1}$] direction as shown by Figure 3. The comparison of the unit cell size obtained in the present work (coincident with X-ray values obtained at the same temperature), see Table 1, with the value reported from X-ray data at room temperature, $a = 19.369(4)$, $b = 6.499(1)$, and $c = 5.084(1)$ Å,[8] shows the existence of anisotropy in the thermal contraction. The largest variation is observed along the direction perpendicular to the cleavage (100) planes and the smallest along *b*. From the strong anisotropy observed in the (100) planes in the 295−370 K range, Szotstak et al. assumed that the transition at approximately 365 K is connected with reorientation of the aggregates.[49] The comparison of the present results with room-temperature X-ray data[7,8] would indicate an

(49) Szostak, M. M.; Jakubowski, B.; Komorowska, M. *Mol Cryst. Liq. Cryst.* **1993**, *229*, 7.
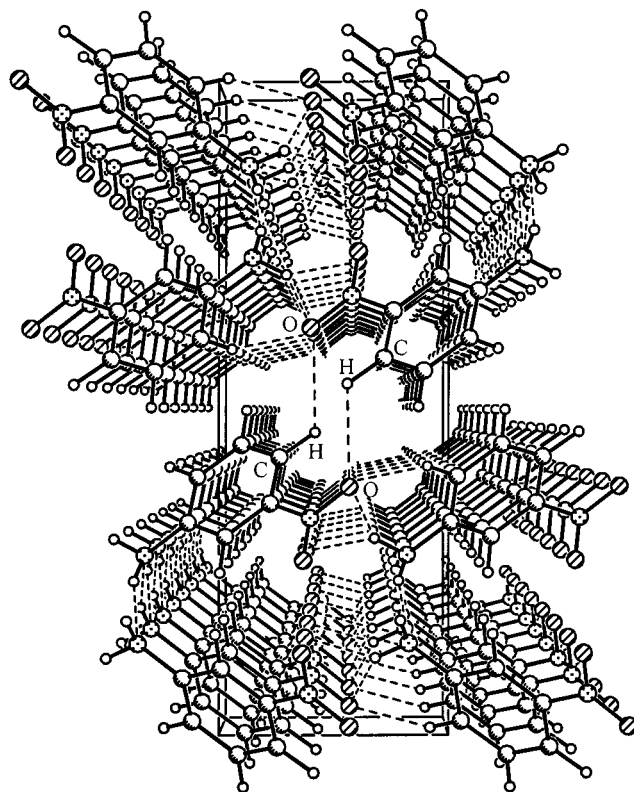

Figure 3. View of mNA along the *c* axis, showing the polar layers perpendicular to [100] and the weak C(ar)−H···O bond linking them.

enhancement of the interactions between the chains forming the ribbons or between the polar layers as the temperature decreases without major changes in the overall three-dimensional molecular arrangement. This might explain the observed phase transition at 160 K as being induced by freezing of molecular vibrations or intermolecular relative motion due to the stronger intermolecular interactions along *a*.

The above-described results provide conclusive evidence that the amino group in nitroanilines might be far from planar and that the amino nitrogen can act as a hydrogen bond acceptor in these systems. They also reinforce the validity of Panunto et al.'s nitroaniline interaction pattern model within the polar chains as this holds even in the presence of a strong pyramidalization of the amine nitrogen, which is the acceptor in the strongest observed hydrogen bond. These findings would also point to the existence of some cooperativity effects within the chains, although no enhancement of the molecular conjugation can be seen from the C−N bond lengths (see Table 3).

The observed important nonplanarity of the amino group and its capability to work as a hydrogen bond acceptor in mNA indicate that the amino nitrogen atom presents a high degree of sp^3 character, in contradiction with previous and strongly established models. Our work also draws into focus the fact that in mNA aggregate calculations the results suggested some degree of nonplanarity of the amino group, but this was disregarded as an artifact of the calculation.[3]

Conclusions

The present results confirm the recognition pattern of nitroanilines through bifurcated three-center hydro-

gen bond synthons. They also showed the nonplanarity of the amino group and that the amino nitrogen can function as an acceptor in these systems. These last two facts have not been considered previously but should certainly be taken into account in the future, not only when performing aggregates calculations but also in designing new materials.

Supporting Information Available: Crystallographic information file (CIF) for mNA. This material is available free of charge via the Internet at http://pubs.acs.org.

CM001092U